

NAOJ-Th-Ap 2000, No.27

The Maximum Effect of Thermal Instability on Galactic Outflows

Yutaka Fujita

National Astronomical Observatory, Mitaka, Tokyo 181-8588, Japan

yfujita@th.nao.ac.jp

ABSTRACT

We have investigated steady, radial gas outflows (or winds) from galaxies and the development of thermal instability in the hot gas. In order to see the maximum influence of the instability on the global structure of the galactic outflows, we study inhomogeneous comoving flows and the non-linear fate of the fluctuations in the flows. We compare the results with solutions for homogeneous flows. In the case of supersonic flows, the global structure of inhomogeneous flows is not much different from that of homogeneous flows. However, detailed investigation shows that the average density of inhomogeneous flows decreases faster than that of homogeneous flows, because local thermal instability removes overdense regions in the inhomogeneous flows and reduces the mass flux. We also find that when the gravity of a galaxy is strong, the cold clouds formed from the removed gas are distributed in the galactic halo. In the case of subsonic flows, the form of inhomogeneous flows is different from that of homogeneous flows near the regions where the flows terminate. The density rise appearing near the regions where the homogeneous flows terminate is not seen in the inhomogeneous flows because the local thermal instability decreases the mass flux. The cold clouds formed through thermal instability in the inhomogeneous flow almost all coast to the same maximum radius.

Subject headings: galaxies: ISM—ISM: jets and outflows—ISM: kinematics and dynamics

1. Introduction

Some observations suggest that gas clouds in and out of galaxies are related to outflows from the galaxies.

In the Galactic halo, there are clouds of neutral hydrogen with a velocity greater than $\sim 80 \text{ km s}^{-1}$; they are called high velocity clouds. There has been an argument about the origin. One idea is that they result from outflows from the Galaxy; thermal instability in the flows leads to cloud formation (Shapiro and Field 1976; Bregman 1980; Li and Ikeuchi 1992). The other is that

they are made from metal-poor gas falling from the outside of the Galaxy (Oort 1970; Blitz, et al. 1999). Recently, however, Richter, et al. (1999) found that the iron abundance in a high velocity cloud in the Galactic halo is half of the solar value, which supports the former idea.

Recent observations of Ly α absorption system show that the absorbers are associated with galaxies (Morris, et al. 1993; Lanzetta, et al. 1995; Stocke, et al. 1995; Bowen, Blades and Pettini 1996; Le Brun, Bergeron and Boisse 1996; van Gorkom, et al. 1996; Chen, et al. 1998). For example, the spectroscopy and broadband imaging of galaxies toward 3C 273 indicate that the Ly α absorbers are not distributed at random with respect to the galaxies (Morris, et al. 1993). Lanzetta, et al. (1995) found an anticorrelation between Ly α absorption equivalent width and galaxy impact parameter. Moreover, metals have been found in the absorption system, which means that the gas is enriched by the products of stellar nucleosynthesis (Rauch 1998). These observations suggest that the absorbers are made from the gas ejected from galaxies. In this case, thermal instability in the outflows is expected to play an important role in the formation of the absorbers.

Wang (1995a) investigated cooling gas outflows from galaxies. He studied the outflow form, the effects of the galaxy potential, the size of outflow regions, and the efficiency of radiative cooling. He found that the hot gas in dwarf galaxies can either flow out as galactic winds, or cool radiatively to form clouds. In the latter case, the clouds can escape from the galaxies and may become Ly α absorbers (Wang 1995b). Recently, Nulsen, Barcons and Fabian (1998) also indicated that the ejected gas from dwarf galaxies can give rise to a damped Ly α absorber. In contrast, Wang (1995a) found that massive galaxies like our own tend to confine the gas; the gas released into the halo either cools radiatively or results in a galactic corona.

However, Wang (1995a) considered only spherical homogeneous flows. (Here, homogeneous means that density and radius from the galaxy center have a one-to-one correspondence.) In actual galaxies, however, there should be density fluctuations that lead to local thermal instabilities. Balbus and Soker (1989) examined the linear evolution of the local thermal instabilities in outflows and found that the growth is relatively weak. On the other hand, the non-linear evolution is not understood well, although complex gas structures observed in galaxies suggest the fluctuations in outflows are highly non-linear (e.g. Jogee, Kenney and Smith 1998). Although there are simulations done to study the non-linear evolution of instability (e.g. Krtsuk, Böhringer and Muller 1998), they cannot resolve fine structure of gas such as shells of supernova remnants and gas blobs composed by mass-loss gas from stars; their scales are typically ~ 10 pc and ~ 1 pc, respectively (Mathews 1990). If these fluctuations grow through radiative cooling, the overdensities condense and are decoupled from outflows. Thus, the substantial quantities of gas may be removed from the outflows, and the form of outflows may be changed. As an instance similar to this one, X-ray observations suggest that a large amount of gas is decoupled from cooling inflows in the central regions of clusters and the cooled gas is deposited in the wide region (Fabian 1994). If it happens to be the same in outflows of a galaxy, the clouds born from the decoupled gas may be distributed in a wide range of radius of the galaxy.

However, this consideration may be too simplistic; the motion of overdense regions relative to the ambient gas introduces complication. If gravity induces the relative motion, the overdense regions mix with the ambient gas and cannot cool anymore. Hattori, Yoshida and Habe (1995) numerically showed that the motion strongly depends on magnetic fields; if the magnetic pressure is strong enough, it goes against the gravity and the overdensities can be sustained. Fujita, Fukumoto and Okoshi (1997) estimated that the magnetic pressure could sustain the overdensities in actual galaxies.

In this paper, we consider the non-linear evolution of fluctuations in inhomogeneous outflows of galaxies and its influence on the global structure of outflows. Since it is difficult to treat the non-linear evolution exactly, we first consider the most extreme case. For this purpose, we investigate multiphase comoving flows, in which local thermal instabilities are expected to grow most extremely because the motion of overdense regions relative to the ambient gas is ignored. We compare the results with those of homogeneous flows.

Our paper is organized as follows. In §2 we summarize our models for both homogeneous and inhomogeneous flows. In §3 we give the results of our calculations and describe the differences between homogeneous and inhomogeneous flows. In §4 the fate of the clouds formed in outflows is discussed. Conclusions are given in §5.

2. Models

2.1. Homogeneous Flows

The equations of mass, momentum, and energy conservation in a steady, symmetric flow are

$$\frac{1}{r^2} \frac{d(r^2 \rho u)}{dr} = 0, \quad (1)$$

$$u \frac{du}{dr} = -\frac{1}{\rho} \frac{dp}{dr} - \frac{GM}{r^2}, \quad (2)$$

$$\frac{\rho u}{\gamma - 1} \frac{d}{dr} \ln \left(\frac{p}{\rho^\gamma} \right) = -n_p^2 \Lambda(T), \quad (3)$$

where ρ , u , p , are respectively the density, velocity, and pressure of the gas, γ is the adiabatic index, G is the gravitational constant, $M(r)$ is the gravitating mass within r , n_p is the proton density, Λ is the cooling function, and T is the temperature. These equations can be rewritten as dimensionless equations for the Mach number and the dimensionless temperature (equations [2.14] and [2.15] in Wang 1995a).

2.2. Inhomogeneous Flows

The model adopted here is based on the multiphase cooling flow model of Nulsen (1986). Contrary to the model of Nulsen (1986), we consider outflows with relatively large velocity.

Using the volume distribution function $f(\rho, \mathbf{r}, t)$ at time, t , and position, \mathbf{r} , the mass within the volume dV , in the density range ρ to $\rho + d\rho$ is given by

$$dM = \rho f(\rho, \mathbf{r}, t) d\rho dV. \quad (4)$$

Differentiating (4), we obtain the equation of mass conservation

$$\frac{\partial \rho f}{\partial t} + \nabla \cdot \rho \mathbf{v} f + \frac{\partial \rho f \dot{\rho}}{\partial \rho} = 0, \quad (5)$$

where $\dot{\rho} = d\rho/dt$ is the comoving rate of change of the density of gas with density ρ , and \mathbf{v} is the velocity. From now on, we assume that the flow is steady and spherically symmetric for simplicity.

The mass flux function Ψ is defined by

$$\Psi(\rho, r) = \int_0^\rho 4\pi r^2 \rho' u f d\rho', \quad (6)$$

where u is the outward radial velocity. As mentioned in §1, we assume that the cooling gas comoves, which means that u is a function of r alone. Thus, there is no local relative motion between gas blobs before they are decoupled from the flow. From equation (5), it can be shown that Ψ satisfies the relation

$$\dot{\rho} \frac{\partial \Psi}{\partial \rho} = -u \frac{\partial \Psi}{\partial r} \quad (7)$$

(see Nulsen 1986). Thus, Ψ is constant along streamlines in the ρ, r plane.

We assume local pressure equilibrium, that is, pressure, p , is also a function of r alone. In this case, the streamlines for the cooling gas are determined from two equations; one is the energy equation

$$\rho T u \frac{dS}{dr} = -n_p^2 \Lambda(T), \quad (8)$$

and the other is the momentum equation

$$u \frac{du}{dr} = -\frac{1}{\bar{\rho}} \frac{dp}{dr} - \frac{GM(r)}{r^2}, \quad (9)$$

where S is the entropy. The temperature is given by the ratio of p to ρ (or n_p). We assume that the cooling function is described by

$$\Lambda = DT^\alpha, \quad (10)$$

where D and α are constants. The spatially averaged density is given by

$$\bar{\rho} = \Psi(\infty, r) / \int_0^\infty \frac{1}{\rho} \frac{\partial \Psi}{\partial \rho} d\rho. \quad (11)$$

The total mass flow rate, \dot{M} , is given by $\dot{M} = 4\pi r^2 \bar{\rho} u$.

We can integrate equation (8) and give

$$(p^{0.6}/\rho)^{2-\alpha} = p_1^{0.6(2-\alpha)} (\rho_i^{-(2-\alpha)} - \rho_c^{-(2-\alpha)}) , \quad (12)$$

where ρ is the density at radius r of the gas with density ρ_i at radius r_1 , $p = p(r)$, $p_1 = p(r_1)$ and $\rho_c(r)$ is the density of the gas at r_1 which just has infinite density at radius r . The evolution of cooling gas along the streamlines is determined by ρ_c . Using equation (12), equation (8) is described by ρ_c

$$u \frac{d}{dr} \rho_c^{2-\alpha} = (2-\alpha) \frac{n_{p1}^2 D T_1^\alpha}{2.5 p_1} \rho_1^{-(2-\alpha)} \left(\frac{p}{p_1} \right)^{0.2+0.4\alpha} , \quad (13)$$

where n_{p1} is the number density corresponding to arbitrary density ρ_1 , and T_1 is the temperature of gas at pressure p_1 and density ρ_1 .

The energy and momentum equations can be solved by assuming the functional form of Ψ . According to Nulsen (1986), we consider two cases. One is a power-law form

$$\Psi(\rho, r_1) = \begin{cases} A(1-w)^k, & w < 1 \\ 0, & w \geq 1 , \end{cases} \quad (14)$$

where

$$w = (\rho/\rho_m)^{-(2-\alpha)} \quad (15)$$

for some constant ρ_m . Assuming that $k \geq 1$, we obtain

$$\bar{\rho} = (p/p_1)^{0.6} J \rho_m (1-w_c)^{-1/(2-\alpha)} , \quad (16)$$

where

$$J = \binom{k+1/(2-\alpha)}{k} \quad (17)$$

and

$$w_c = (\rho_c/\rho_m)^{-(2-\alpha)} . \quad (18)$$

Thus, equation (9) and (13) can be rewritten as

$$\frac{d}{dr} \left(\frac{p}{p_1} \right) = - \frac{J \rho_m}{p_1} \left(\frac{p}{p_1} \right)^{0.6} (1-w_c)^{-1/(2-\alpha)} \left(u \frac{du}{dr} + \frac{GM}{r^2} \right) \quad (19)$$

and

$$\frac{d}{dr} (1-w_c) = (2-\alpha) \frac{4\pi r^2 \rho_m J}{At_{cm}} \left(\frac{p}{p_1} \right)^{0.8+0.4\alpha} (1-w_c)^{-k-1/(2-\alpha)} , \quad (20)$$

where t_{cm} is the constant pressure cooling time evaluated for $r = r_1$ and $\rho_1 = \rho_m$ (or $n_{p1} = n_{pm}$ if represented by number density), that is,

$$t_{cm} = \frac{5p_1}{2n_{pm}^2 D T_1^\alpha} . \quad (21)$$

Since total mass flow rate is $\dot{M} = A(1 - w_c)^k$, equations (19) and (20) are respectively given by

$$\frac{d}{dr} \left(\frac{p}{p_1} \right) = -\frac{J\rho_m}{p_1} \left(\frac{p}{p_1} \right)^{0.6} \left(\frac{\dot{M}}{\dot{M}_1} \right)^{-1/k(2-\alpha)} \left(u \frac{du}{dr} + \frac{GM}{r^2} \right) \quad (22)$$

and

$$\frac{d}{dr} \dot{M} = -k(2 - \alpha) \frac{4\pi r^2 \rho_m J}{t_{cm}} \left(\frac{p}{p_1} \right)^{0.8+0.4\alpha} \left(\frac{\dot{M}}{\dot{M}_1} \right)^{-1/k-1/k(2-\alpha)}, \quad (23)$$

where $\dot{M}_1 = \dot{M}(r_1)$. Using equation (16), we obtain

$$u = \frac{\dot{M}}{4\pi r^2 \bar{\rho}} = \frac{\dot{M}}{4\pi r^2 J \rho_m} \left(\frac{p}{p_1} \right)^{-0.6} \left(\frac{\dot{M}}{\dot{M}_1} \right)^{1/k(2-\alpha)}. \quad (24)$$

Thus, equations (22) and (23) are simultaneous equations for p and \dot{M} .

The other form of Ψ is an exponential form,

$$\Psi(\rho, r_1) = A e^{-w}. \quad (25)$$

As is the case of the power-law form (equation [14]), we have the momentum equation

$$\frac{d}{dr} \left(\frac{p}{p_1} \right) = -\frac{L\rho_m}{p_1} \left(\frac{p}{p_1} \right)^{0.6} \left(u \frac{du}{dr} + \frac{GM}{r^2} \right) \quad (26)$$

and the energy equation

$$\frac{d}{dr} \dot{M} = -(2 - \alpha) \frac{4\pi r^2 \rho_m L}{t_{cm}} \left(\frac{p}{p_1} \right)^{0.8+0.4\alpha}, \quad (27)$$

where

$$L = \frac{1}{(1/(2 - \alpha))!}. \quad (28)$$

3. Results

According to Wang (1995a), we adopt the cooling function for a gas with solar metal abundance,

$$\Lambda(T) = 6.2 \times 10^{-19} (T/K)^{-0.6} \text{ cm}^3 \text{ s}^{-1} \quad (29)$$

(McKee and Cowie 1977; Sutherland and Dopita 1993). This is a good approximation at $10^5 \lesssim T \lesssim 4 \times 10^7$ K. Note that this cooling function may not be appropriate to study the formation of Ly α absorbers because their observed abundance is about 1/100 solar. However, although the absolute value of the cooling function with the abundance is about one tenth of that of equation (29), the temperature dependence is not much different from -0.6 for $T \lesssim 10^6$ K (Sutherland and

Dopita 1993). Thus, the evolution of the flow with solar abundance is similar to that with 1/100 solar abundance and three or four times larger gas density, because their local cooling times are almost identical.

For a model galaxy, we consider the isothermal mass distribution

$$\frac{GM}{r} = v_{\text{cir}}^2 \quad (30)$$

with truncated radius r_{max} . We consider both supersonic and subsonic flows. The Mach number of flows, \mathcal{M} , is taken as unity at the base of the flows. As discussed by Wang (1995a), it is a natural choice at least for the initial condition in supersonic flows, because a smooth transition from a subsonic flow at the center to a supersonic flow at large radius requires that $\mathcal{M} = 1$ at $r = R$, where R is the radius beyond which heating ceases (Chevalier and Clegg 1985). The parameters of model galaxies are the same as those in Wang (1995a) and are shown in Table 1. Model D1 corresponds to a typical dwarf galaxy in which the gas tends to flow out. Model N1 corresponds to a massive galaxy like our own in which the gas tends to be confined. Models D2 and N2 are the same as models D1 and N2, respectively, but the initial gas temperature and the total mass flow rate are larger. For the power-law type of mass flux function (equation [14]), we take $k = 2$ but the results are not much different even if we take $k = 10$.

3.1. Supersonic Flows

As an initial condition, we take $\mathcal{M} = 1 + \epsilon$ ($\epsilon \sim 10^{-3} - 10^{-4}$) at the inner boundary r_i . Since the results for models D2 and N2 are qualitatively similar to those for model D1, we present only the results for models D1 and N1 here. In Figures 1 and 2, we show the profiles of pressure, density, temperature, velocity, and the ratio of cooling to flow time. For inhomogeneous flows, we plot the average density (equation [11]), and the average temperature given by the ratio of the pressure to the average density. The cooling time and flow time are defined by

$$t_c = \frac{P}{(\gamma - 1)n_p^2 \Lambda(T)} \quad (31)$$

and

$$t_f = \frac{r}{v} \quad (32)$$

respectively. In equation (31), we use the averaged density and temperature for inhomogeneous flows. In Figures 1 and 2, we also show the total mass flow rate, \dot{M} , for inhomogeneous flows.

For homogeneous flows, in model D1 (and D2, N2) hot gas flows out of the galaxy (Figure 1d), while in model N1 the hot gas is confined, although the gas is first accelerated by pressure (Figure 2d). We define a dimensionless variable

$$x = \frac{\rho v_{\text{cir}}^2}{4\pi(r/v_{\text{cir}})n_p^2 \Lambda(T)} \quad (33)$$

That is, $1/x$ is the fraction of the energy loss due to radiation during the flow time r/v_{cir} for a flow with velocity equal to the rotation velocity of the galaxy (Wang 1995a). At the initial radius r_i , $x \sim 1$ in model N1 and $x < 1$ in others. This means that galactic gravitational potential is important in model N1 while it is not important in others, which explains the characteristics of the homogeneous outflows. Since initially $t_c > t_f$ in model N1, the gas first cools adiabatically; radiative cooling becomes dominant later on ($t_c < t_f$). Note that in model D1 although t_c/t_f also becomes smaller than one for $r \gtrsim 3$ kpc for homogeneous flow (Figure 1e), the gas temperature of the flow has already been smaller than 10^5 K at $r \sim 2$ kpc (Figure 1c), that is, equation (29) should not be adopted there.

Broadly speaking, the profiles of pressure, average density, average temperature, and velocity of the hot gas for inhomogeneous flows are similar to those for homogeneous flows. However, it is shown that the gas pressure and density for the inhomogeneous flows decrease rather faster than those for the homogeneous flows (Figures 1 and 2). This is because of the decrease of the mass flux (equations [23] and [27]). In fact, Figures 1f and 2f show that \dot{M} decreases outwardly, reflecting that thermal instability removes overdense regions from the flows. In model D1, in the region where \dot{M} decreases ($r \gtrsim 1$ kpc), the terms of pressure gradient and gravity in equation (9) are small and the gas expands freely ($u \sim \text{constant}$). Thus, the decrease of \dot{M} reduces $\bar{\rho}$ because $\bar{\rho} = \dot{M}/(4\pi r^2 u)$. In model N1, in the region where \dot{M} decreases ($r \gtrsim 7$ kpc), the gravity term in equation (9) dominates the pressure gradient term. This means that the velocity u is determined only by the gravitational field and does not depend on the homogeneity of the flow. Thus, the decrease of \dot{M} reduces $\bar{\rho}$ as is the case of model D1. It is to be noted that even in the region where $t_c/t_f > 1$, \dot{M} decreases (Figures 1 and 2), because t_c is defined for the averaged density and the overdense regions in the flows cool ahead of most of the gas.

3.2. Subsonic Flows

The initial conditions for subsonic flows are the same as those of the supersonic flows except for the initial velocity; we take $\mathcal{M} = 1 - \epsilon$ ($\epsilon \sim 10^{-3} - 10^{-4}$) at the inner boundary r_i . We present the results for models D1 and N1; the results for other models are qualitatively the same as those for model D1.

Although gas is confined in a galaxy for all models, the solutions for inhomogeneous flows are different from those for homogeneous flows (Figures 3 and 4). The density increase appearing near the regions where the homogeneous flows terminate does not exist for the inhomogeneous flows. Figures 3 and 4 show that t_c/t_f decreases rapidly because the velocity of the flows reduces. Thus, radiative cooling becomes important and causes gas condensation near the regions where the homogeneous flows terminate. On the other hand, for inhomogeneous flows, radiative cooling makes mass-dropout effective and prevents the density increase from appearing.

In model N1 in §3.1 and in the models discussed in this subsection, radiatively cooled gas

piles up at finite distances from a galaxy. This appears to be inconsistent with the assumption of steady flows. However, if the cold gas turns into dense, compact clouds, the clouds ballistically fall back to the galaxy and the gas accumulation does not significantly affect the global structure of the outflows unless they are disrupted and mix with ambient gas soon after the formation. The stability of the clouds have been studied by many authors. For example, although the clouds are subject to Kelvin-Helmholtz instability, Murray, et al. (1993) indicated that the clouds are stable for a long time if they are bound by a sufficiently strong (self-)gravitational potential. Moreover, Hattori and Umetsu (2000) indicated that the evaporation of the clouds by surrounding hot gas may be greatly suppressed by a plasma instability. In the next section, we discuss the motion of the clouds including the case that the gravity of a galaxy cannot stop outflows.

4. Discussion

We assume that cooled gas in outflows turns to be stable clouds, which move ballistically. The initial velocity of the newly formed clouds is expected to be the velocity of the flow at the position of their formation if the formation time-scale is small enough. We consider whether the clouds escape from a galaxy or fall back under the influence of the galactic potential.

Since the mass distribution of our model galaxy is truncated at radius r_{\max} , the escape velocity is given by

$$v_{\text{esc}}(r) = \sqrt{2} v_{\text{cir}} \left[1 + \ln \left(\frac{r_{\max}}{r} \right) \right] \quad (34)$$

for $r < r_{\max}$. We take $r_{\max} = 50 r_i$ from now on. If the clouds cannot escape from the galaxy, the maximum radius they can reach is given by

$$r_f = r_c \exp \left[\frac{1}{2} \left(\frac{v_c}{v_{\text{cir}}} \right)^2 \right], \quad (35)$$

if $r_f \leq r_{\max}$, or

$$r_f = \frac{2v_{\text{cir}}^2}{v_{\text{esc}}^2(r_c) - v_c^2} r_{\max}, \quad (36)$$

if $r_f > r_{\max}$, where v_c is the velocity of clouds when they form at radius r_c (Wang 1995a). In equations (35) and (36), we assume that $r_c < r_{\max}$. For all the models adopted here, this relation is satisfied.

Figures 5 and 6 show the relation between r_c and r_f for supersonic and subsonic flows, respectively. First, we discuss supersonic flows. Since in models D1, D2, and N2, the clouds can escape from the galaxy regardless of the position where they are born, we discuss only model N1. For the homogeneous flow, assuming that clouds form when the temperature of gas drops to $\sim 10^5$ K, the clouds cannot escape from the galaxy (Figure 5). For the inhomogeneous flows, the clouds also cannot escape but r_f has a distribution. The clouds that form nearer to the galaxy center have smaller r_f . By comparing Figure 5 with Figure 2, it is shown that about two third of the clouds

formed from the inhomogeneous flows have the orbit which is almost the same as the clouds formed from the homogeneous flow ($r_f \sim 40$ kpc); other clouds have smaller apocentric radii.

Second, we consider subsonic flows. For homogeneous flows, the initial velocity of clouds is almost zero, if we assume that they form when the temperature of gas drops to $\sim 10^5$ K. Thus, the clouds start to fall back to the galaxy immediately. For inhomogeneous flows, most of the clouds cannot escape from the galaxy, although the clouds that form near to r_i can escape in models D1 and D2 (Figure 6). Contrary to the supersonic flows in model N1 (Figure 5), the clouds that form nearer to the galaxy have larger r_f in models D1, D2, and N2, because v_c is a strong decreasing function of r . However, in model D1 for example, in spite of the wide distribution of r_f , it can be shown that more than 90% of the gas which originally composed of the outflow can coast only to $r_f \sim 1$ kpc by comparing Figure 6a with Figure 3f. This can be said to other models as well; most of the gas dropped out of the flow reaches the almost same radius ($r_f \sim 1$ kpc for model D2 and $r_f \sim 10$ kpc for models N1 and N2). Moreover, the subsonic flows cannot explain the observed correlation between galaxies and Ly α absorbers because their separations range 12.4 to $157.4h^{-1}$ (Chen, et al. 1998).

The clouds formed in the galactic halo fall back toward the galaxy. For our model galaxy, a cloud with velocity zero at radius r_f has infall velocity,

$$v_{\text{fall}} = v_{\text{cir}} \sqrt{2 \ln \left(\frac{r_f}{r_{\text{fall}}} \right)}, \quad (37)$$

at radius r_{fall} if $r_f < r_{\text{max}}$. When $v_{\text{cir}} = 225$ km s $^{-1}$ and $r_f = 10$ kpc, $v_{\text{fall}} = 128$ km s $^{-1}$ at $r_{\text{fall}} = 8.5$ kpc. Thus, the observed high velocity clouds may be related to the clouds formed from the subsonic flows.

5. Conclusions

We study thermal instability in galactic outflows (or winds) and its effect on the global structure of the outflows. In order to investigate the maximum effect, we consider comoving inhomogeneous (multiphase) outflows in which overdense regions move together with ambient gas; comoving flows may be possible if magnetic fields are strong enough.

We formulate the inhomogeneous flow and apply it to dwarf galaxies and normal galaxies. We compared the results with solutions for homogeneous flows. For supersonic flows, the pressure, density, temperature, and velocity profiles of hot gas for homogeneous and those for inhomogeneous flows are similar. However, strictly speaking, the density of inhomogeneous flows decreases somewhat faster than that of homogeneous flows as the gas expands. This is because local thermal instability removes overdensities from the flows owing to local gas condensation. On the other hand, for subsonic flows, solutions for inhomogeneous flows are significantly different from those of homogeneous flows near the regions where the flows terminate. While radiative cooling and

gas condensation raise gas density near the regions where the homogeneous flows terminate, local thermal instability in the inhomogeneous flows removes overdensities and prevents an upturn of the average density.

The gas radiatively cooled is most likely to form clouds. The newly formed clouds inherit the velocity of a flow at the position of their formation if the time-scale of the formation is much smaller than the flow time-scale. For supersonic flows, we find that the clouds can escape from dwarf galaxies regardless of the homogeneity of flows. On the other hand, for massive galaxies like our own, the clouds cannot escape from the galaxies without an extreme starburst; in particular, the model of an inhomogeneous supersonic flow predicts that the clouds are widely distributed in a galactic halo. For subsonic flows, most of the clouds are confined in galaxies regardless of the homogeneity of flows and the galaxy mass. Most of the clouds formed in an inhomogeneous flow reach the almost same radius before being pulled back by gravitation.

Although the assumption of comoving flows may be too extreme and the effect of thermal instability estimated here may be too strong, we think that this possibility cannot be ruled out at present.

I am grateful to K. Okoshi and S. Inutsuka for useful discussions. Comments from an anonymous referee led to significant improvements in the quality of this paper.

REFERENCES

Balbus, S. A. and Soker, N. 1989, *ApJ*, 341, 619
Blitz, L., Spergel, D. N., Teuben, P. J., Hartmann, D. and Burton, W. B. 1999, *ApJ*, 514, 818
Bowen, D. V., Blades, J. C. and Pettini, M. 1996, *ApJ*, 464, 141
Bregman, J. N. 1980, *ApJ*, 236, 577
Chen, H., Lanzetta, K. M., Webb, J. K. and Barcons, X. 1998, *ApJ*, 498, 77
Chevalier, R. A., and Clegg, A. W. 1985, *Nature*, 317, 44
Fabian, A. C. 1994, *ARA&A*, 32, 277
Fujita, Y., Fukumoto, J. and Okoshi, K. 1997, *ApJ*, 488, 585
Hattori, M. and Umetsu, K. 2000, *ApJ*, 533, 84
Hattori, M., Yoshida, T. and Habe, A. 1995, *MNRAS*, 275, 1195
Jogee, S., Kenney, J. D. P. and Smith, B. J. 1998, *ApJ*, 494, L185

Kritsuk, A., Böhringer, H. and Muller, E. 1998, MNRAS, 301, 343

Lanzetta, K. M., Bowen, D. B., Tytler, D. and Webb, J. K. 1995, ApJ, 442, 538

Le Brun, V., Bergeron, J. and Boisse, P. 1996, A&A, 306, 691

Li, F. and Ikeuchi, S. 1992, ApJ, 390, 405

Mathews, W. G. 1990, ApJ, 354, 468

McKee, C. F. and Cowie, L. L. 1977, ApJ, 215, 213

Morris, S. L., Weymann, R. J., Dressler, A., McCarthy, P. J., Smith, B. A., Terrile, R. J., Giovanelli, R. and Irwin, M. 1993, ApJ, 419, 524

Murray, S. D., White, S. D. M., Blondin, J. M. and Lin, D. N. C. 1993, ApJ, 407, 588

Nulsen, P. E. J. 1986, MNRAS, 221, 377

Nulsen, P. E. J., Barcons, X. and Fabian, A. C. 1998, MNRAS, 301, 168

Oort, J. H. 1970, A&A, 7, 381

Rauch, M. 1998, ARA&A, 36, 267

Richter, P., de Boer, K. S., Widmann, H., Kappelmann, N., Gringel, W., Grewing, M. and Barnstedt, J. 1999, Nature, 402, 386

Shapiro, P. R. and Field, G. B. 1976, ApJ, 205, 76

Stocke, J. T., Shull, J. M., Penton, S., Donahue, M. and Carilli, C. 1995, ApJ, 451, 24

Sutherland, R. S. and Dopita, M. 1993, ApJS, 88, 253

van Gorkom, J. H., Carilli, C. L., Stocke, J. T., Perlman, E. S. and Shull, J. M. 1996, AJ, 112, 1397

Wang, B. 1995a, ApJ, 444, 590

Wang, B. 1995b, ApJ, 444, L17

Table 1. Model Parameters.

Models	v_{cir} (km s $^{-1}$)	r_i (kpc)	T_i (K)	$\dot{M}(r_i)$ (M $_{\odot}$ yr $^{-1}$)
D1	50	0.3	3×10^6	0.3
D2	50	0.3	2×10^7	10
N1	225	3	3×10^6	3
N2	225	3	2×10^7	100

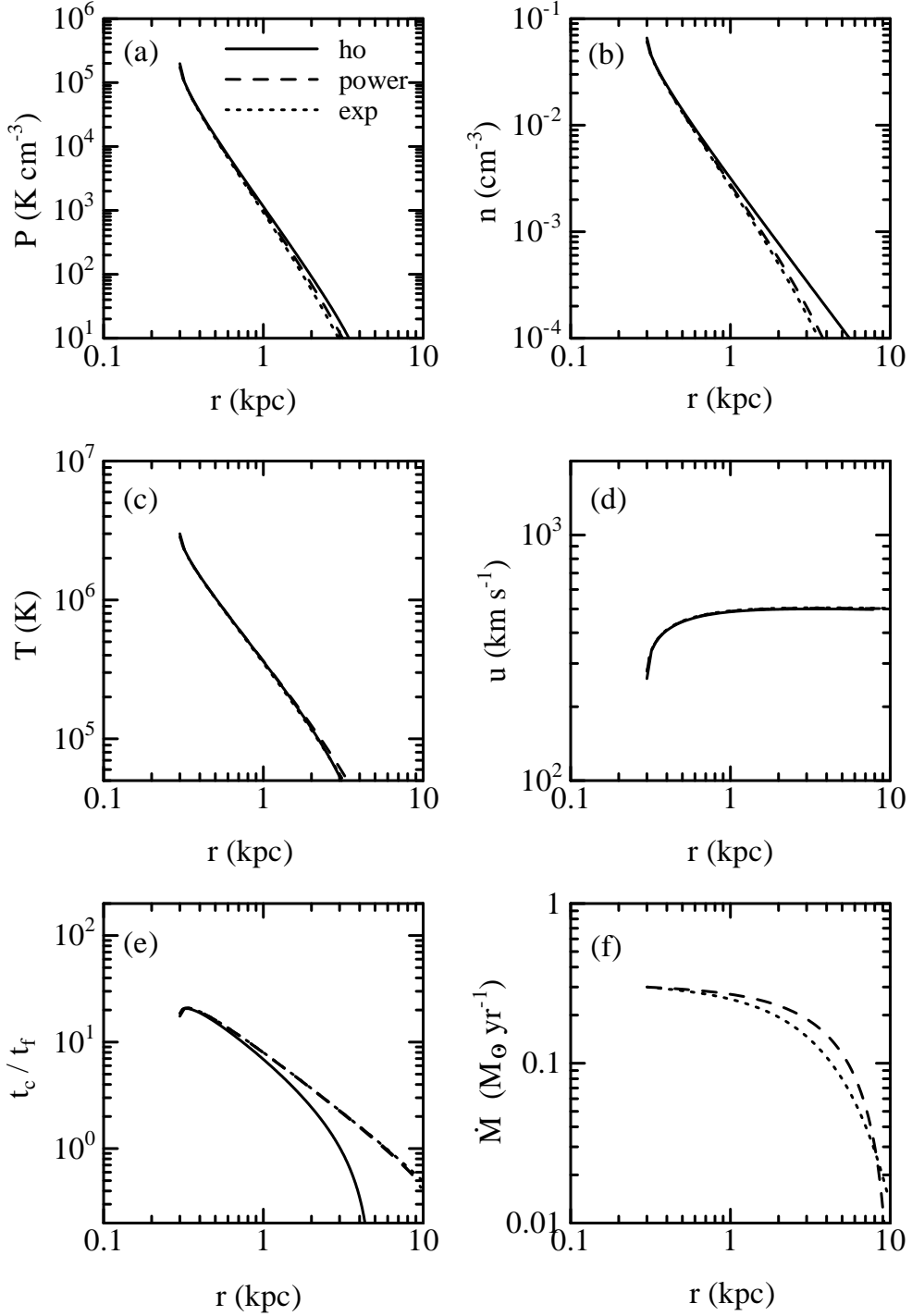


Fig. 1.— (a) Gas pressure, (b) number density, (c) temperature, (d) velocity, (e) ratio of the cooling time and the flow time, and (f) total mass flux as functions of radius for supersonic flows in model D1. The solid lines indicate homogeneous flows. The dashed and dotted lines respectively indicate inhomogeneous flows with the power-law mass-flux function (equation [14]; $k = 2$) and those with the exponential mass-flux function (equation [25]).

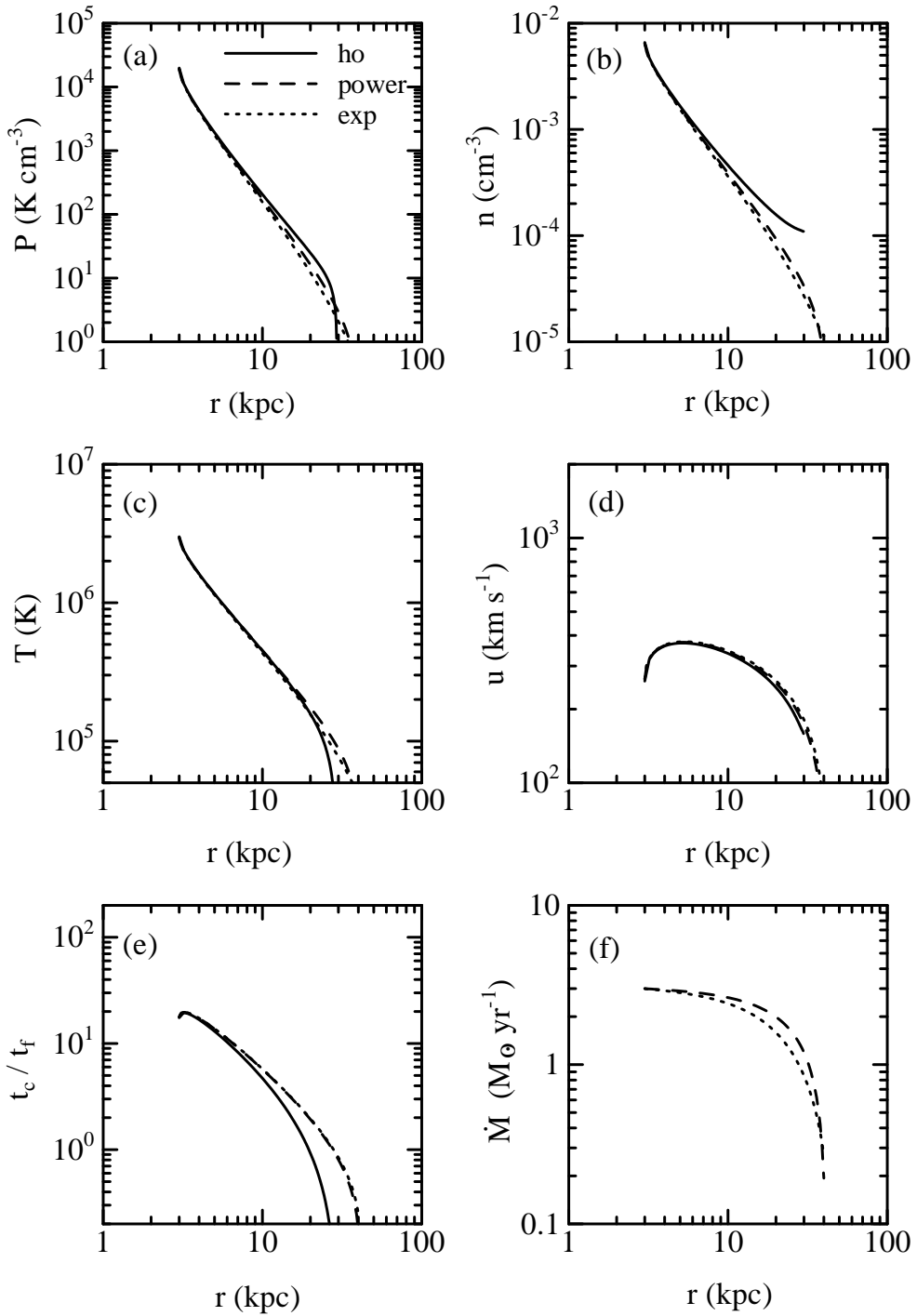


Fig. 2.— The same as Figure 1 but for supersonic flows in model N1.

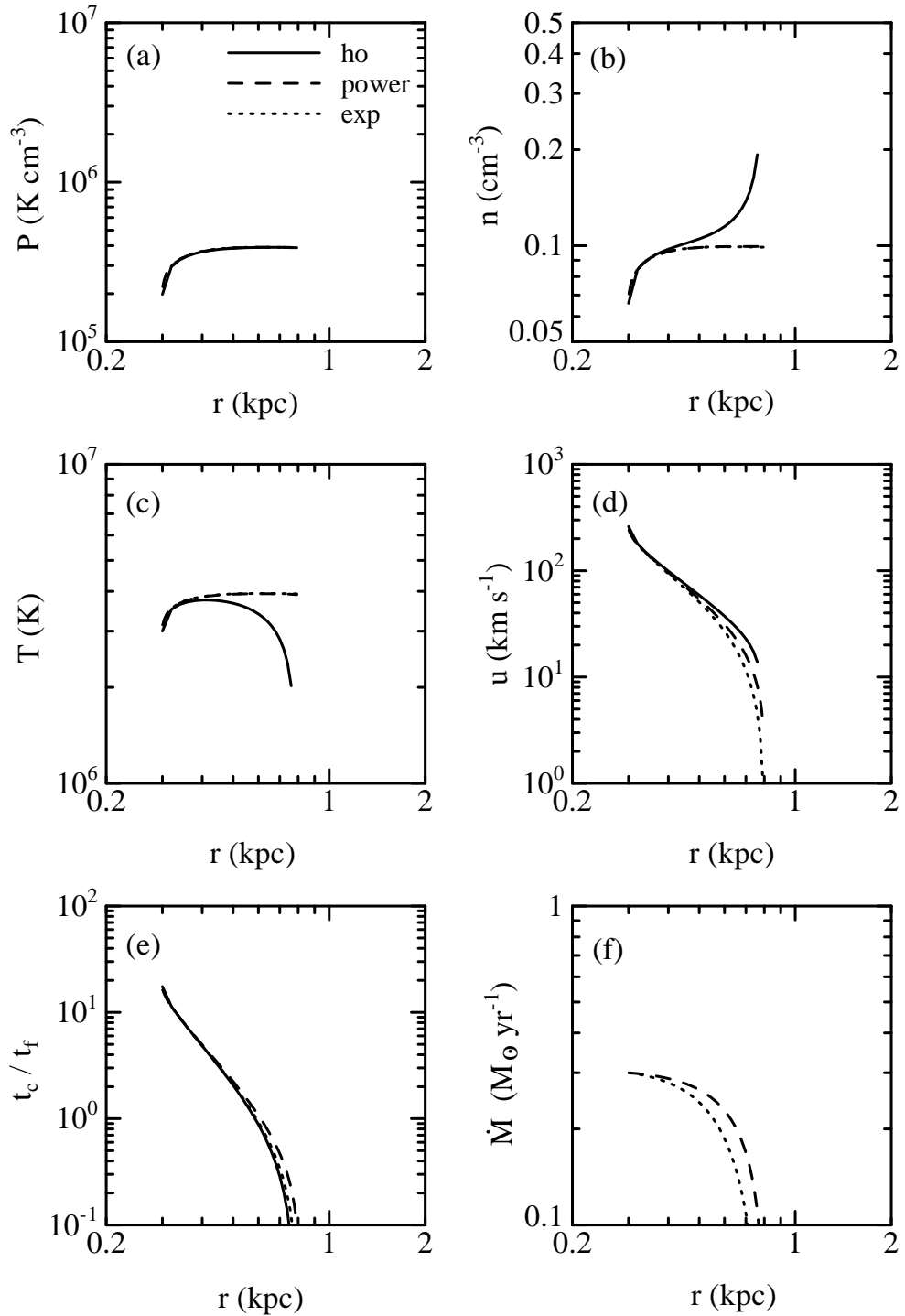


Fig. 3.— The same as Figure 1 but for subsonic flows in model D1.

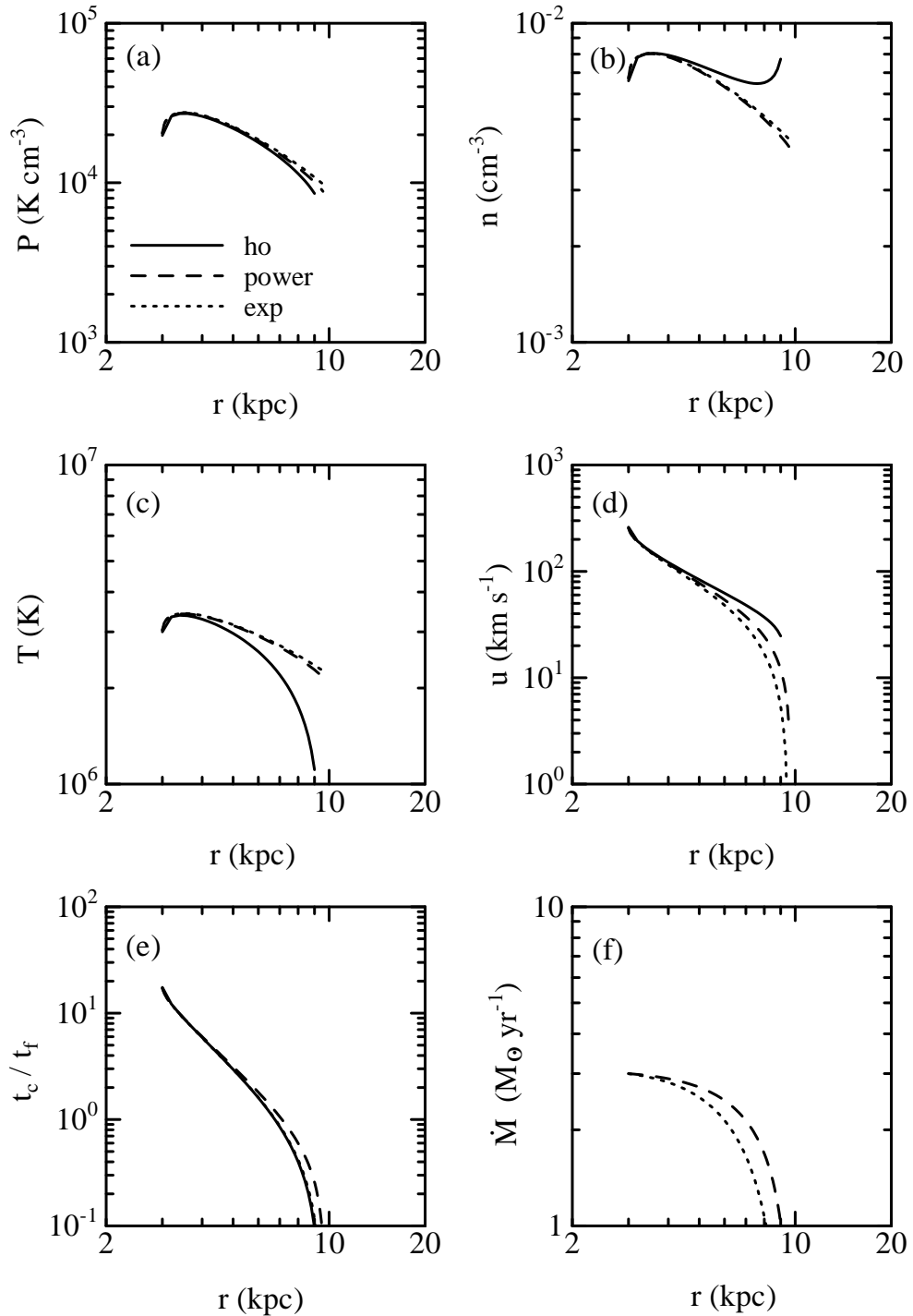


Fig. 4.— The same as Figure 1 but for subsonic flows in model N1.

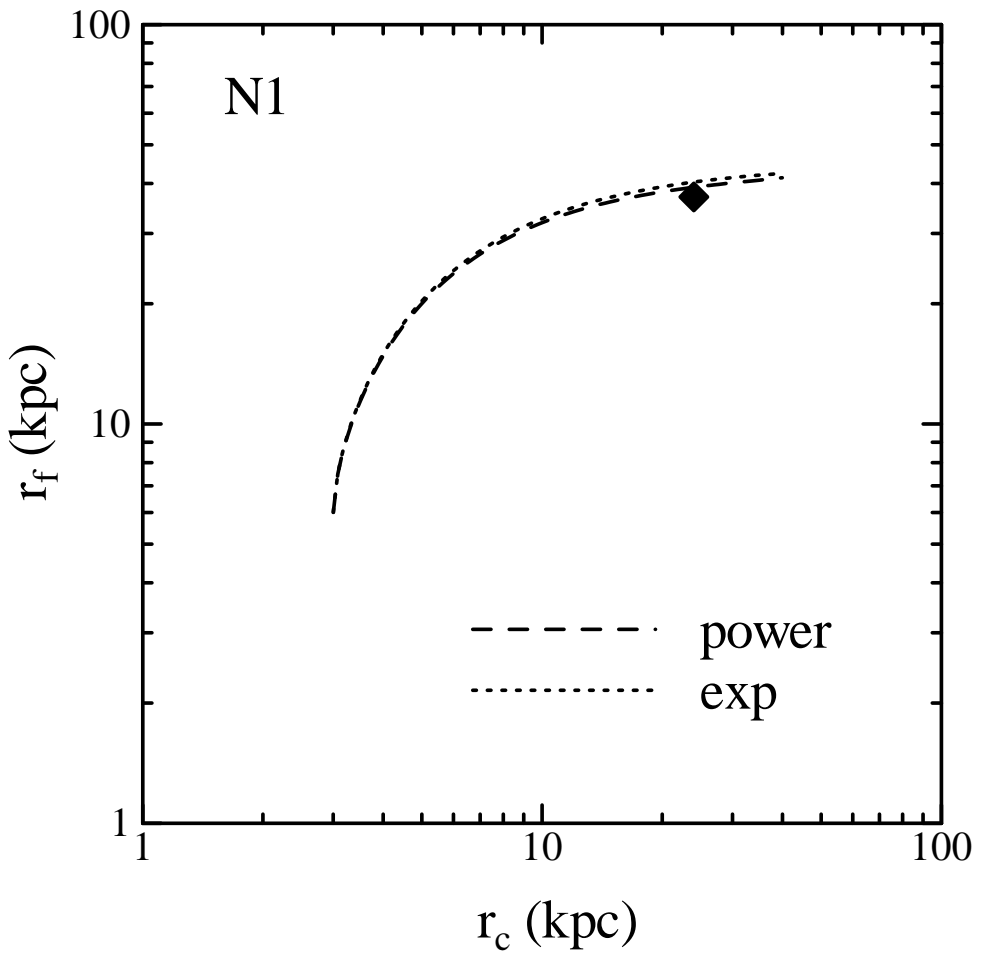


Fig. 5.— The relation between the position where clouds form and the position where the clouds reach for supersonic flows in model N1. The dashed and dotted lines respectively indicate inhomogeneous flows with the power-law mass-flux function (equation [14]; $k = 2$) and those with the exponential mass-flux function (equation [25]). The diamond shows the result for the homogeneous flow.

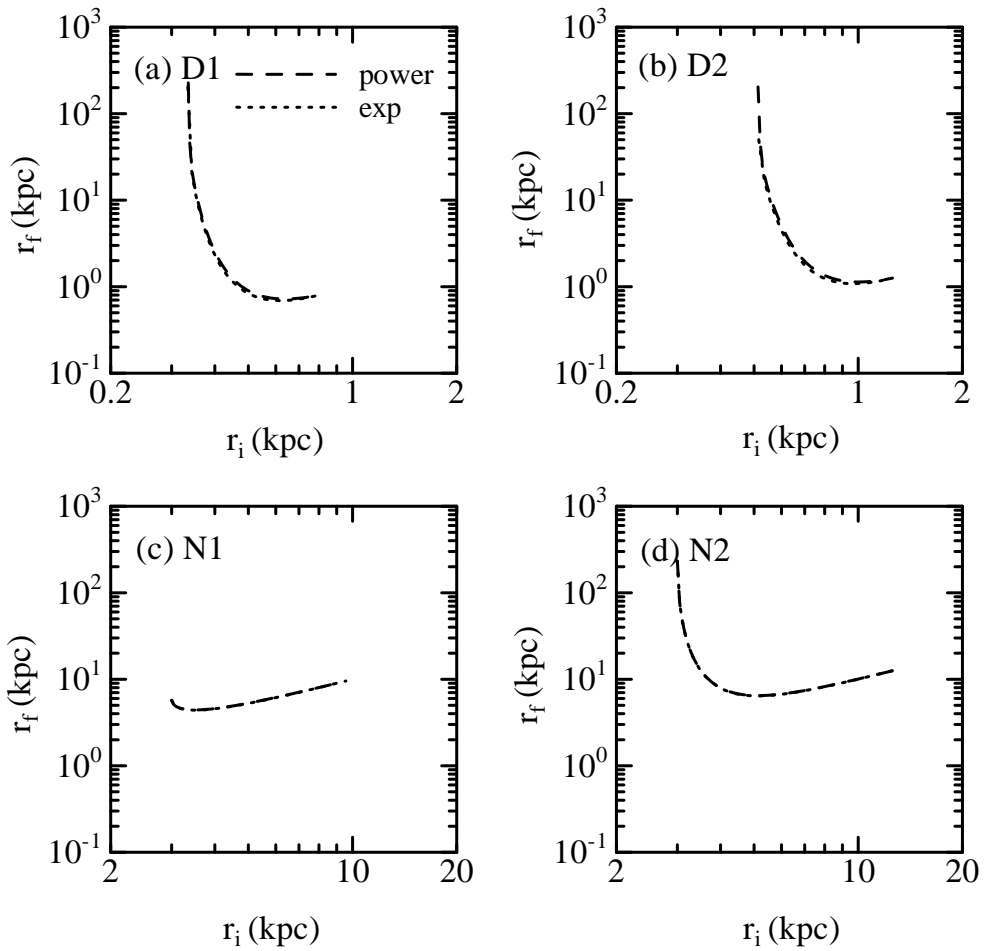


Fig. 6.— The relation between the position where clouds form and the position where the clouds reach for supersonic flows. The dashed and dotted lines respectively indicate inhomogeneous flows with the power-law mass-flux function (equation [14]; $k = 2$) and those with the exponential mass-flux function (equation [25]). (a) model D1 (b) model D2 (c) model N1 (d) model N2.